Title

Amine Dynamics in Diamine-Appended Mg_2(dobpdc) Metal-Organic Frameworks.

Journal

The journal of physical chemistry letters, 10(22)

ISSN

1948-7185

Authors

Xu, Jun
Liu, Yifei Michelle
Lipton, Andrew S
et al.

Publication Date

2019-11-01

DOI

10.1021/acs.jpclett.9b02883

Peer reviewed

Amine Dynamics in Diamine-Appended Mg_2(dobpdc) Metal–Organic Frameworks

Jun Xu,[ϕ,†,] Yifei Michelle Liu,[†] Andrew S. Lipton,[ϕϕ] Jinxing Ye,[†,‡,ϕϕϕ] Gina L. Hoatson,[∫] Phillip J. Milner,[‡,§] Thomas M. McDonald,[‡,§] Rebecca L. Siegelman,[‡,§] Alexander C. Forse,[†,‡,#] Berend Smit,[†,∫∫] Jeffrey R. Long,[†,‡,§] Jeffrey A. Reimer[†,§]*

[ϕ]Center for Rare Earth and Inorganic Functional Materials, Tianjin Key Lab for Rare Earth Materials and Applications, School of Materials Science and Engineering & National Institute for Advanced Materials, Nankai University, Tianjin 300350, China

[†]Department of Chemical and Biomolecular Engineering, [‡]Department of Chemistry, and [#]Berkeley Energy and Climate Institute, University of California, Berkeley, California 94720, United States

[ϕϕ]Environmental Molecular Sciences Laboratory, Pacific Northwest National Laboratory, 902 Battelle Boulevard, Richland, Washington 99354, United States

[ϕϕϕ]Engineering Research Center of Pharmaceutical Process Chemistry, Ministry of Education, School of Pharmacy, East China University of Science and Technology, 130 Meilong Road, Shanghai 200237, China

[∫]Department of Physics, College of William and Mary, P. O. Box 8795, Williamsburg, Virginia 23187-8795, United States

∬Laboratory of Molecular Simulation, Institut des Sciences et Ingénierie Chimiques, Valais Ecole Polytechnique Fédérale de Lausanne (EPFL), Rue de l'Industrie 17, CH-1951 Sion, Switzerland

§Materials Sciences Division, Lawrence Berkeley National Laboratory, Berkeley, California 94720, United States

*Email: junxu@nankai.edu.cn.

Abstract: Variable-temperature ^{15}N solid-state NMR spectroscopy is used to uncover the dynamics of three diamines appended to the metal–organic framework Mg_2(dobpdc) (dobpdc^{4-} = 4,4′-dioxidobiphenyl-3,3′-dicarboxylate), an important family of CO_2 capture materials. The results imply both bound and free amine nitrogen environments exist when diamines are coordinated to the framework open Mg^{2+} sites. There are rapid exchanges between two nitrogen environments for all three diamines, the rates and energetics of which are quantified by ^{15}N solid-state NMR data and corroborated by density functional theory calculations and molecular dynamics simulations. The activation energy for the exchange provides a measure of the metal−amine bond strength. The unexpected negative correlation between the metal−amine bond strength and CO_2 adsorption step pressure unravel that metal-amine bond strength is not the only important factor in determining the CO_2 adsorption properties of diamine-appended Mg_2(dobpdc) MOFs.

TOC GRAPHIC

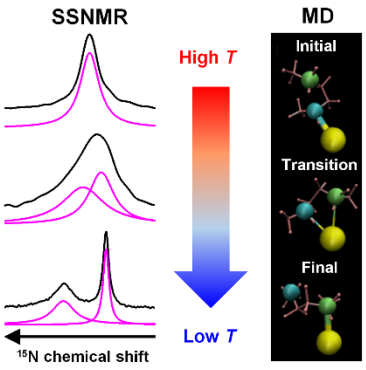

Rising anthropogenic CO_2 emissions remain the leading source of global climate change.[1] The capture and sequestration of CO_2 from power plant flue gas emissions has thus been highlighted as a potentially promising emission mitigation strategy in recent years.[2-4] Numerous approaches have been developed for the removal of CO_2 from flue gas through the use of aqueous amine solutions,[4] zeolites,[5] metal–organic frameworks (MOFs),[6] covalent organic frameworks,[7] *etc.* Among them, MOFs with coordinatively-unsaturated metal centers such as the M_2(dobdc) family (dobdc^{4-} = 2,5-dioxido-1,4-benzenedicarboxylate; M = Mg, Mn, Fe, Co, Ni, Cu, Zn) have attracted considerable attention due to the strong interaction that occurs between the metal centers and CO_2 upon adsorption, which leads to a high affinity for CO_2 adsorption and selectivity over N_2.[8-12] One drawback of these materials, however, is that their performance often diminishes under humid conditions.[13-15] Later, it was demonstrated that after grafting diamines onto the coordinatively-unsaturated metal sites of M_2(dobpdc) (dobpdc^{4-} = 4,4′-dioxidobiphenyl-3,3′-dicarboxylate), the expanded analogues of M_2(dobdc), the resulting material can exhibit substantially improved CO_2 adsorption performances arising from step-shaped adsorption isotherms (or isobars) that allow for high working capacities during temperature- or pressure-swing adsorption processes and robust performance under humid conditions.[15-20] Notably, the step pressure (or temperature) can be tuned through variation of the structure of appended diamines,[16-20] and it is therefore of fundamental

importance to investigate in detail the influence of diamine structure on the CO_2 adsorption properties of diamine-appended Mg_2(dobpdc) materials..

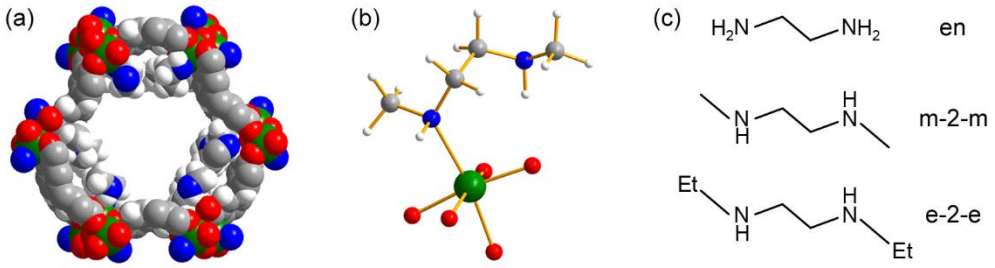

Figure 1. (a) Space-filling model of Mg_2(dobpdc) appended with *N*,*N*′-dimethylethylenediamine, m-2-m–Mg_2(dobpdc), and (b) Ball-and-stick model of an m-2-m-appended Mg^{2+} site within the framework, with both metal-bound and free nitrogen environments. The models are taken from the DFT-optimized structures reported in this work. Green, red, blue, grey, and white spheres represent Mg, O, N, C, and H atoms, respectively. And all other H atoms are omitted for clarity. (c) The structures of three diamines studied in this work.

Diamine-appended variants of Mg_2(dobpdc), such as the *N*,*N*′-dimethylethylenediamine (m-2-m)-appended framework (Figure 1), presume to have one nitrogen coordinated to Mg^{2+}, while the other amine group extends into the open MOF pore.[16, 18] Above a threshold pressure (or below a threshold temperature), CO_2 inserts into the Mg−N bond, yielding a carbamate group bound to Mg^{2+} and an ammonium group at the other end of the diamine (Figure S1, Supporting Information). Electrostatic interaction between the negative carbamate and a neighboring positive ammonium triggers the synergistic formation of ammonium–carbamate chain along the framework channel, inducing the observed cooperative adsorption behavior.[16, 18, 21] As a consequence, the metal–amine bond strength may play an important role in determining the pressure or temperature at which CO_2 insertion occurs. This effect has been examined recently via single-crystal X-ray diffraction (XRD) characterization of the isostructural diamine-appended Zn_2(dobpdc) frameworks,[18] which readily

form single crystals. Even still, these single-crystal structures consist of a large degree of diamine disorder within the framework channels at 100 K, and so it is essential to develop additional approaches for assessing the structures, particularly for the diamine-appended Mg_2(dobpdc) variants. We were specifically interested in exploring the dynamic behavior of the diamines within the MOF pores, as a potential means of guiding the design of new diamine-appended structures for CO_2 capture. Since the dissociation of Mg−N bond is a pre-requisite for diamine dynamics, the magnitude of activation energy can be used to estimate the Mg−N bond strength. If the insertion of CO_2 into Mg−N bond is the most important factor for step-shaped adsorption, weaker Mg−N bond should result in lower step pressure.

Solid-state NMR (SSNMR) spectroscopy is a characterization technique complementary to the diffraction-based techniques such as XRD and it is very sensitive to the local environment and dynamics around the observed nucleus. ^{13}C and ^{17}O SSNMR data have been used to probe the CO_2 dynamics in M_2(dobdc) MOFs and uncover strong interactions between CO_2 and coordinatively-unsaturated metal centers.[22-24] In the case of diamine-appended Mg_2(dobpdc), the subtle difference between metal-bound and free nitrogen environments of diamines should be detectable by ^{15}N SSNMR spectroscopy.[25-26] Although the ^{15}N SSNMR spectrum of m-2-m–Mg_2(dobpdc) was previously found to exhibit a single ^{15}N peak at ambient temperature,[16] a recent ^{25}Mg SSNMR study implied that the two nitrogen environments undergo rapid exchange, inducing a significant disorder of local magnesium environment.[27] Herein, we analyze variable-temperature (VT) ^{15}N SSNMR data to probe local nitrogen environments and dynamics of three ^{15}N-labelled diamines appended to MOF Mg_2(dobpdc) (diamine/Mg ≈ 1/1), namely ethylenediamine (en, 98 atom% ^{15}N), *N*,*N*′-dimethylethylenediamine (m-2-m, ~50 atom% ^{15}N), and *N*,*N*′-diethylethylenediamine (e-2-e, ~20 atom% ^{15}N). In each sample, the SSNMR data enable the elucidation of diamine dynamics

within framework channels, yielding activation energies for diamine exchange that provide a measure of the metal−amine bond strength. When combined with density functional theory (DFT) calculations and molecular dynamics (MD) simulations, these results provide insights into correlations between diamine structure and the CO_2 adsorption properties of these materials.

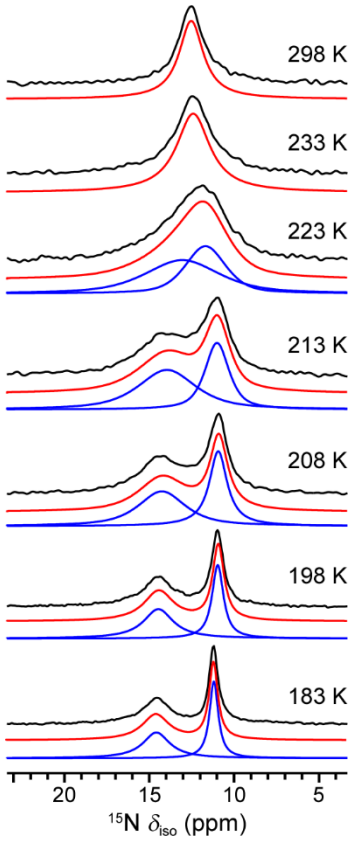

Figure 2. ^{15}N direct-polarization (DP) SSNMR spectra of en–Mg_2(dobpdc) at 20.0 T as a function of temperature. Black, blue, and red profiles are experimental, deconvoluted, and the summation of deconvoluted spectra, respectively. The signal intensities are normalized for clarity. The recycle delays were calibrated to ensure the sufficient relaxation of ^{15}N.

We first observed the trend of change in ^{15}N SSNMR spectra of en–Mg_2(dobpdc) as a function of temperature (Figure 2). Herein, all ^{15}N chemical shift values were referenced to neat NH_3(l) at

0 ppm. In en–Mg_2(dobpdc), the high ^{15}N enrichment degree (98 atom%) enabled acquisition of high-quality direct-polarization (DP) spectra. At 298 K, a symmetric ^{15}N peak arises at 12.7 ppm. This peak broadens considerably upon cooling to 233 K and then becomes asymmetric at 223 K, eventually separating into two peaks upon further cooling. The separation between these two new peaks continues to increase with decreasing temperature, while their characteristic line widths (*i.e.*, the full-width-at-half-maximum, FWHM) decrease. At the lowest measurement temperature of 183 K, the two peaks are observed at 14.8 and 11.4 ppm, respectively. This overall trend as a function of temperature is consistent with the exchange between two nitrogen environments.[28-32] We assigned the peak at 14.8 ppm to the metal-bound amine nitrogen environment and the peak at 11.4 ppm to the free amine nitrogen environment, respectively. The bonding interactions between Mg^{2+} and amine nitrogen result in deshielding of ^{15}N (*i.e.*, a larger ^{15}N chemical shift value is observed), verified by DFT calculations (Figure S6).

Deconvolution of ^{15}N SSNMR spectra enables determination of the frequency separation between two ^{15}N peaks as well as their line widths, and from this information it is possible to calculate a chemical exchange rate constant. For example, in the range where the peak positions exhibit a strong temperature dependence (*i.e.*, 223–208 K), the exchange rate constant k_E was calculated using the equation $k_E = \pi\sqrt{(\Delta\nu_o^2 - \Delta\nu_e^2)}/\sqrt{2}$, where $\Delta\nu_o$ is the frequency separation between the two peaks (in Hz) without exchange and $\Delta\nu_e$ is the separation with exchange.[28-32] The exchange rate constant k_E was found to be 3.16×10^2 s^{-1} at 213 K, and the calculation details for all k_E values (Table S3) are shown in Supporting Information Section S5.

It has been reported that the N-alkylation of en enables the tuning of CO_2 adsorption properties of diamine-appended Mg_2(dobpdc).[16-20] We thus used the same VT ^{15}N SSNMR analyses to assess

the dynamics of m-2-m and e-2-e appended to MOF Mg_2(dobpdc). For the two samples, the lower ^{15}N enrichment degree (~50 atom% for m-2-m and ~20 atom% for e-2-e, respectively) makes acquisition of high-quality DP spectra challenging. ^{1}H–^{15}N cross-polarization (CP) spectra were acquired instead. The quality of CP spectra is typically better than DP spectra but they are less quantitative. In this work, both CP and DP spectra exhibit the same trend of change (Figure S12 and Figure S13) thus only high-quality CP spectra were employed in data analyses. At 293 K, the spectrum of m-2-m consists of an asymmetric peak at 13.3 ppm and a weak shoulder at ~20 ppm (Figure 3a). Upon cooling, the asymmetric peak narrows and shifts to the more shielded region of the spectrum (*i.e.*, a lower ^{15}N chemical shift value). This peak can be deconvoluted into two components at all temperatures, and at 193 K the deconvoluted peaks occur at 16.7 and 15.7 ppm for the metal-bound and free amine nitrogen environments, respectively. The chemical shift value of the shoulder is close to that of the single ^{15}N peak observed for free m-2-m in toluene (Figure S14), and is assigned to the unbound diamine trapped in MOF pores. It is noteworthy that both metal-bound and free amine ^{15}N peaks are shielded compare to the unbound diamine, implying the proximity of corresponding nitrogen atoms to the aromatic rings of dobpdc^{4-} linkers and thus experiencing significant ring-current effects.[33] Characterization of a second m-2-m–Mg_2(dobpdc) sample verified the above-mentioned peak assignments as well as the changes in peak position as a function of temperature (Figures S12 and S14). At higher temperature (313 K), a symmetric ^{15}N peak was indeed observed, implying fast exchange of nitrogen environments of m-2-m.

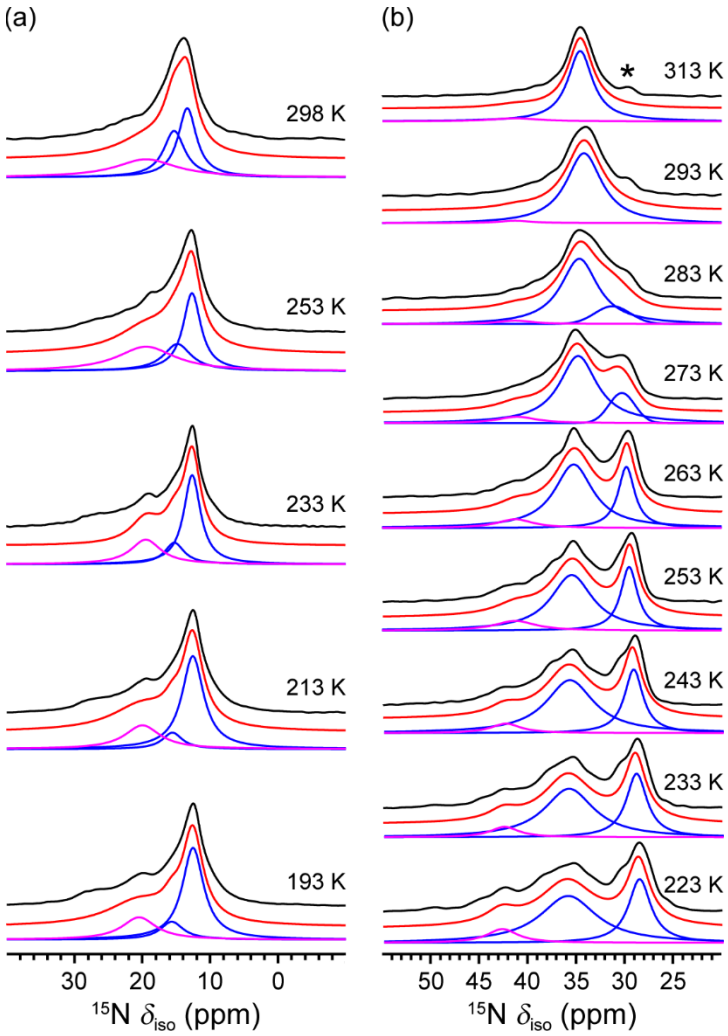

Figure 3. ^{1}H–^{15}N cross-polarization (CP) SSNMR spectra of m-2-m–Mg_2(dobpdc) (a) and e-2-e–Mg_2(dobpdc) (b) as a function of temperature. Black profiles are experimental spectra. Blue and pink profiles are deconvoluted spectra. Red profiles are the summation of deconvoluted spectra. Pink profiles represent the ^{15}N signals that were assigned to unbound diamines trapped in the MOF pores. All signal intensities are normalized for clarity. The asterisk in the 313 K data of e-2-e–Mg_2(dobpdc) is an artifact. The recycle delays were calibrated to ensure the sufficient relaxation of ^{1}H.

The observed trend of changes in VT ^{15}N SSNMR spectra of e-2-e–Mg_2(dobpdc) is remarkably different. As Figure 3b illustrates, at 313 K, a single ^{15}N peak appears at 34.6 ppm and becomes

asymmetric at 283 K, eventually splitting into two peaks upon further cooling. The peak separation increased with decreasing temperature, and at the lowest measured temperature (223 K), the two resulting peaks were at 36.0 and 28.7 ppm, assigned to the metal-bound and free amine nitrogen environments, respectively. Similar to m-2-m–Mg_2(dobpdc), a weak shoulder was present at ~40 ppm at all temperatures, attributed to unbound e-2-e in the pores (Figure S14). For both samples, these diamines were found not to participate in the exchange (see Figure S15 and the following discussions). The frequency separation between the metal-bound and free amine nitrogen peaks increased considerably even at the lowest measurement temperature for both m-2-m–Mg_2(dobpdc) and e-2-e–Mg_2(dobpdc). The precise frequency separation (in Hz) without exchange $\Delta\nu_o$ and the exchange rate constant k_E for the two samples are thus not available in the current work. However, we can still calculate the maximum possible E_A values, assuming the exchange is in the slow limit regime at the lowest measurement temperature. The calculation of these data (Table S3) along with additional discussions can be found in Supporting Information Section S5.

We then applied Arrhenius analysis to determine the activation energy for exchange between the metal-bound and free amine nitrogen environments, on the basis of the rate constants measured in ^{15}N SSNMR experiments. The results are shown in Table 1. A much larger activation energy E_A was found for en (37 ± 2 kJ·mol^{-1}) appended to Mg_2(dobpdc) than for m-2-m and e-2-e (the maximum possible E_A is 6.4 ± 1.5 and 10.9 ± 0.9 kJ·mol^{-1} for m-2-m and e-2-e, respectively), indicating that the substitution of an amine hydrogen with an alkyl group (*i.e.*, changing the metal-bound amine from primary to secondary) significantly weakens the metal–amine bond. The observed trend of change is consistent with the reported single-crystal XRD data for the Zn analogues,[18] in which both primary/secondary and primary/tertiary diamines coordinate to Zn^{2+} centers preferentially through the primary amine.

Table 1. Activation energies (E_A) and step pressures for CO_2 insertion at 393 K of three diamines appended to Mg_2(dobpdc).

Diamine	E_A (kJ·mol^{-1})		Step Pressure (mbar)
	Experimental	Calculated	
en	37 ± 2		30[19]
m-2-m	6.4 ± 1.5[a]	7.93 ± 1.41	200[18]
e-2-e	10.9 ± 0.9[a]	10.5 ± 1.3	50[18]

a: It is the maximum possible E_A value, calculated by assuming the exchange is in the slow limit regime at the lowest measurement temperature.

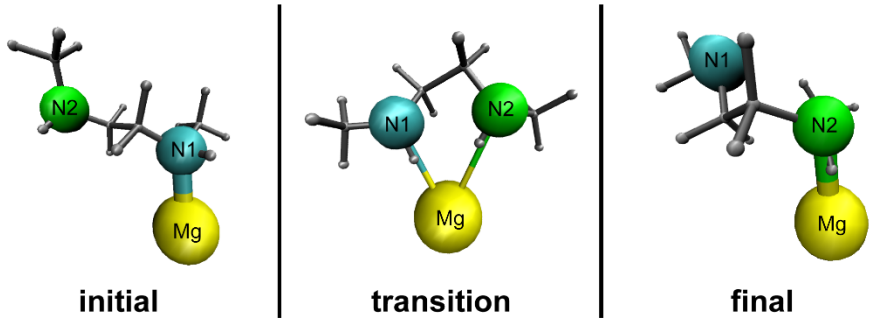

Figure 4. Still frames from the MD trajectory illustrating representative initial, transition, and final states for the amine nitrogen atoms in an m-2-m exchange event. In the transition state, the nitrogen that is initially unbound (N2) coordinates to the Mg^{2+} center, and in the final state the initially bound nitrogen (N1) becomes free.

Molecular dynamics (MD) simulations have been extensively used to study the flexibility and guest dynamics in various MOFs,[23, 27, 34-37] and we employed this approach to further examine the dynamics and compute the exchange rate constant for the diamines appended to Mg_2(dobpdc). In order to capture the bond breakage and formation in the exchange event, we employed the ReaxFF, a reactive force field based on bond order.[34, 38] The simulation results confirm exchange between the metal-bound and free amine nitrogen environments for m-2-m and e-2-e (see Figure 4, Figure

S7, and the movie in the Supporting Information) and enable identification of a possible exchange mechanism, with a transition state with both nitrogen atoms of the diamine molecule weakly bound to the same Mg^{2+} center. However, the simulation did not yield exchange for en, implying that it is still not perfect. The kinetic activation energy E_A for m-2-m and e-2-e calculated from MD simulations have similar magnitudes as the maximum possible E_A measured in NMR experiments and both E_A values are much smaller than the experimental E_A value for en (Table 1).

As previously elucidated, the first step in proposed CO_2 adsorption mechanism in these diamine-appended materials is the insertion of CO_2 into metal−amine bonds (Figure S1).[16, 21] Because the metal−amine bonds are broken upon CO_2 insertion, stronger bonds and therefore higher activation energies for nitrogen exchange are expected to correlate with higher adsorption step pressures (or lower step temperatures). The opposite trend was observed experimentally, with step pressure for en–Mg_2(dobpdc) significantly lower than those of m-2-m– and e-2-e–Mg_2(dobpdc), despite the larger activation barrier toward nitrogen environment exchange for en compared to m-2-m and e-2-e.[16-19] Therefore, it seems that other factors can also influence the thermodynamics of adsorption remarkably,[18] such as the enthalpy of formation of carbamate and the loss of rotational and vibrational degrees of freedom upon ammonium−carbamate chain formation (*i.e.*, a large negative entropy change).

In conclusion, we used variable-temperature ^{15}N SSNMR spectroscopy to probe the coexistence of metal-bound and free amine nitrogen environments in three diamine-appended variants of the Mg_2(dobpdc) metal–organic framework, and further identified a likely transition state involved in nitrogen exchange from MD simulations. The magnitude of the activation energies extracted from SSNMR experiments afforded a measure of metal−amine bond strength, indicating that m-2-m–

and e-2-e–Mg_2(dobpdc) materials have similar bond strengths and both are weaker than that for en–Mg_2(dobpdc). The trends in the experimental data were verified by DFT calculations and MD simulations, and all together the data imply that the metal−amine bond strength is not the only important determiner of CO_2 adsorption step pressure. The approach described herein can be importantly extended to other diamine-appended metal–organic frameworks to understand diamine dynamics and CO_2 adsorption, toward the design of carbon capture materials with improved performances.

ASSOCIATED CONTENT

Supporting Information. Additional information including elucidated CO_2 adsorption mechanism, sample preparation, characterizations, theoretical calculations, rate constant calculations and additional discussions. DFT-optimized structures. Movie of diamine exchange. The following files are available free of charge via the Internet at http://pubs.acs.org.

Electronic Supporting Information (PDF)

DFT-optimized Structure (CIF)

Movie of diamine exchange (MPG)

AUTHOR INFORMATION

Corresponding Author

*Email: junxu@nankai.edu.cn.

Notes

The authors declare the following competing financial interest(s): T.M.M. and J.R.L. have a financial interest in Mosaic Materials, Inc., a start-up company working to commercialize metal–

organic frameworks for gas separations. UC Berkeley has applied for a patent on some of the materials discussed herein, on which T.M.M. and J.R.L. are included as inventors.

ACKNOWLEDGMENT

This work was supported through the Center for Gas Separations Relevant to Clean Energy Technologies, an Energy Frontier Research Center funded by the U.S. Department of Energy, Office of Science, Basic Energy Sciences, under Award DE-SC0001015. Some ^{15}N SSNMR experiments were performed at the Environmental Molecular Sciences Laboratory, a DOE Office of Science User Facility sponsored by the Office of Biological and Environmental Research. DFT calculations were performed at the Molecular Graphics and Computation Facility at UC Berkeley, which is funded by the U.S. National Institutes of Health under Award S10OD023532. The MD simulations were carried out at the National Energy Research Scientific Computing Center, a User Facility supported by the Office of Science of the U.S. Department of Energy under Contract DE-AC02-05CH11231. Y.M.L. thanks the NSF Graduate Research Fellowship program. P.J.M. thanks the National Institute of General Medical Sciences of the National Institutes of Health for a postdoctoral fellowship. J.X. acknowledges the financial support from the National Natural Science Foundation of China (Project 21904071) and the Open Funds (KF1818) of the State Key Laboratory of Fine Chemicals. We thank Dr. Jeffrey Martell for experimental assistance and fruitful discussions, and Dr. Katie Meihaus for editorial assistance.

REFERENCES

(1) IPCC. Contributions of Working Group I to the Fifth Assessment Report of the Intergovernmental Panel on Climate Change. In *Climate Change 2013: The Physical Science Basis*, Stocker, T. F.; Qin, D.; Plattner, G.-K.; Tignor, M. M. B.; Allen, S. K.; Boschung, J.; Nauels, A.; Xia, Y.; Bex, V.; Midgley, P. M., Eds. Cambridge University Press: Cambridge, United Kingdom and New York, 2013.

(2) IPCC. *IPCC Special Report on Carbon Dioxide Capture and Storage*. Cambridge University Press: Cambridge, United Kingdom and New York, 2005.

(3) Bhown, A. S.; Freeman, B. C. Analysis and Status of Post-Combustion Carbon Dioxide Capture Technologies. *Environ. Sci. Technol.* **2011,** *45*, 8624–8632.
(4) Schimming, V.; Hoelger, C.-G.; Buntkowsky, G.; Sack, I.; Fuhrhop, J.-H.; Rocchetti, S.; Limbach, H.-H. Evidence by ^{15}N CPMAS and $^{15}N–^{13}C$ REDOR NMR for Fixation of Atmospheric CO_2 by Amino Groups of Biopolymers in the Solid State. *J. Am. Chem. Soc.* **1999,** *121*, 4892-4893.
(5) Choi, S.; Drese, J. H.; Jones, C. W. Adsorbent Materials for Carbon Dioxide Capture from Large Anthropogenic Point Sources. *ChemSusChem* **2009,** *2*, 796-854.
(6) Sumida, K.; Rogow, D. L.; Mason, J. A.; McDonald, T. M.; Bloch, E. D.; Herm, Z. R.; Bae, T.-H.; Long, J. R. Carbon Dioxide Capture in Metal–Organic Frameworks. *Chem. Rev.* **2012,** *112*, 724-781.
(7) Zeng, Y.; Zou, R.; Zhao, Y. Covalent Organic Frameworks for CO_2 Capture. *Adv. Mater.* **2016,** *28*, 2855-2873.
(8) Rosi, N. L.; Kim, J.; Eddaoudi, M.; Chen, B.; O'Keeffe, M.; Yaghi, O. M. Rod Packings and Metal–Organic Frameworks Constructed from Rod-Shaped Secondary Building Units. *J. Am. Chem. Soc.* **2005,** *127*, 1504-1518.
(9) Dietzel, P. D. C.; Blom, R.; Fjellvåg, H. Base-Induced Formation of Two Magnesium Metal–Organic Framework Compounds with a Bifunctional Tetratopic Ligand. *Eur. J. Inorg. Chem.* **2008,** *2008*, 3624-3632.
(10) Caskey, S. R.; Wong-Foy, A. G.; Matzger, A. J. Dramatic Tuning of Carbon Dioxide Uptake via Metal Substitution in a Coordination Polymer with Cylindrical Pores. *J. Am. Chem. Soc.* **2008,** *130*, 10870-10871.
(11) Yazaydin, A. O.; Snurr, R. Q.; Park, T.-H.; Koh, K.; Liu, J.; LeVan, M. D.; Benin, A. I.; Jakubczak, P.; Lanuza, M.; Galloway, D. B.; Low, J. J.; Willis, R. R. Screening of Metal–Organic Frameworks for Carbon Dioxide Capture from Flue Gas Using a Combined Experimental and Modeling Approach. *J. Am. Chem. Soc.* **2009,** *131*, 18198-18199.
(12) Wu, H.; Zhou, W.; Yildirim, T. High-Capacity Methane Storage in Metal–Organic Frameworks M_2(dhtp): The Important Role of Open Metal Sites. *J. Am. Chem. Soc.* **2009,** *131*, 4995-5000.
(13) Kizzie, A. C.; Wong-Foy, A. G.; Matzger, A. J. Effect of Humidity on the Performance of Microporous Coordination Polymers as Adsorbents for CO_2 Capture. *Langmuir* **2011,** *27*, 6368-6373.
(14) Yu, J.; Balbuena, P. B. Water Effects on Postcombustion CO_2 Capture in Mg-MOF-74. *J. Phys. Chem. C* **2013,** *117*, 3383-3388.
(15) Mason, J. A.; McDonald, T. M.; Bae, T.-H.; Bachman, J. E.; Sumida, K.; Dutton, J. J.; Kaye, S. S.; Long, J. R. Application of a High-Throughput Analyzer in Evaluating Solid Adsorbents for Post-Combustion Carbon Capture via Multicomponent Adsorption of CO_2, N_2, and H_2O. *J. Am. Chem. Soc.* **2015,** *137*, 4787−4803.
(16) McDonald, T. M.; Mason, J. A.; Kong, X.; Bloch, E. D.; Gygi, D.; Dani, A.; Crocella, V.; Giordanino, F.; Odoh, S. O.; Drisdell, W. S.; Vlaisavljevich, B.; Dzubak, A. L.; Poloni, R.; Schnell, S. K.; Planas, N.; Lee, K.; Pascal, T.; Wan, L. F.; Prendergast, D.; Neaton, J. B.; Smit, B.; Kortright, J. B.; Gagliardi, L.; Bordiga, S.; Reimer, J. A.; Long, J. R. Cooperative Insertion of CO_2 in Diamine-Appended Metal-Organic Frameworks. *Nature* **2015,** *519*, 303-308.
(17) McDonald, T. M.; Lee, W. R.; Mason, J. A.; Wiers, B. M.; Hong, C. S.; Long, J. R. Capture of Carbon Dioxide from Air and Flue Gas in the Alkylamine-Appended Metal–Organic Framework mmen-Mg_2(dobpdc). *J. Am. Chem. Soc.* **2012,** *134*, 7056-7065.

(18) Siegelman, R. L.; McDonald, T. M.; Gonzalez, M. I.; Martell, J. D.; Milner, P. J.; Mason, J. A.; Berger, A. H.; Bhown, A. S.; Long, J. R. Controlling Cooperative CO_2 Adsorption in Diamine-Appended Mg_2(dobpdc) Metal–Organic Frameworks. *J. Am. Chem. Soc.* **2017,** *139*, 10526-10538.
(19) Lee, W. R.; Hwang, S. Y.; Ryu, D. W.; Lim, K. S.; Han, S. S.; Moon, D.; Choi, J.; Hong, C. S. Diamine-Functionalized Metal-Organic Framework: Exceptionally High CO_2 Capacities from Ambient Air and Flue Gas, Ultrafast CO_2 Uptake Rate, and Adsorption Mechanism. *Energ. Environ. Sci.* **2014,** *7*, 744-751.
(20) Milner, P. J.; Siegelman, R. L.; Forse, A. C.; Gonzalez, M. I.; Runčevski, T.; Martell, J. D.; Reimer, J. A.; Long, J. R. A Diaminopropane-Appended Metal–Organic Framework Enabling Efficient CO_2 Capture from Coal Flue Gas via a Mixed Adsorption Mechanism. *J. Am. Chem. Soc.* **2017,** *139*, 13541-13553.
(21) Vlaisavljevich, B.; Odoh, S. O.; Schnell, S.; Dzubak, A. L.; Lee, K.; Planas, N.; Neaton, J.; Gagliardi, L.; Smit, B. CO_2 Induced Phase Transitions in Diamine-Appended Metal Organic Frameworks. *Chem. Sci.* **2015,** *6*, 5177-5185.
(22) Kong, X.; Scott, E.; Ding, W.; Mason, J. A.; Long, J. R.; Reimer, J. A. CO_2 Dynamics in a Metal–Organic Framework with Open Metal Sites. *J. Am. Chem. Soc.* **2012,** *134*, 14341-14344.
(23) Lin, L.-C.; Kim, J.; Kong, X.; Scott, E.; McDonald, T. M.; Long, J. R.; Reimer, J. A.; Smit, B. Understanding CO_2 Dynamics in Metal–Organic Frameworks with Open Metal Sites. *Angew. Chem. Int. Ed.* **2013,** *52*, 4410-4413.
(24) Wang, W. D.; Lucier, B. E. G.; Terskikh, V. V.; Wang, W.; Huang, Y. Wobbling and Hopping: Studying Dynamics of CO_2 Adsorbed in Metal–Organic Frameworks via ^{17}O Solid-State NMR. *J. Phys. Chem. Lett.* **2014,** *5*, 3360-3365.
(25) Witanowski, M.; Stefaniak, L.; Webb, G. A. Nitrogen NMR Spectroscopy. In *Annual Reports on NMR Spectroscopy*, Webb, G. A., Ed. Academic Press: 1993; Vol. 25, pp 1-480.
(26) Mason, J. Nitrogen NMR. In *Encycl. NMR*, Harris, R. K.; Wasylishen, R. E., Eds. John Wiley & Sons, Ltd: 2012; Vol. 5.
(27) Xu, J.; Blaakmeer, E. S. M.; Lipton, A. S.; McDonald, T. M.; Liu, Y. M.; Smit, B.; Long, J. R.; Kentgens, A. P. M.; Reimer, J. A. Uncovering the Local Magnesium Environment in the Metal–Organic Framework Mg_2(dobpdc) Using ^{25}Mg NMR Spectroscopy. *J. Phys. Chem. C* **2017,** *121*, 19938-19945.
(28) McConnell, H. M. Reaction Rates by Nuclear Magnetic Resonance. *J. Chem. Phys.* **1958,** *28*, 430-431.
(29) Abragam, A. *The Principles of Nuclear Magnetism*. Clarendon Press: Oxford, 1961.
(30) Bain, A. D. Chemical Exchange in NMR. *Prog. Nucl. Magn. Reson. Spectrosc.* **2003,** *43*, 63–103.
(31) Alexander, S. Exchange of Interacting Nuclear Spins in Nuclear Magnetic Resonance. II. Chemical Exchange. *J. Chem. Phys.* **1962,** *37*, 974–980.
(32) Limbach, H.-H.; Wehrle, B.; Schlabach, M.; Kendrick, R.; Yannoni, C. S. CPMAS Polarization Transfer Methods for Superposed Chemical Exchange and Spin Diffusion in Organic Solids. *J. Magn. Reson.* **1988,** *77*, 84-100.
(33) Pople, J. A. Proton Magnetic Resonance of Hydrocarbons. *J. Chem. Phys.* **1956,** *24*, 1111.
(34) Huang, L.; Joshi, K. L.; Duin, A. C. T. v.; Bandosz, T. J.; Gubbins, K. E. ReaxFF Molecular Dynamics Simulation of Thermal Stability of a $Cu_3(BTC)_2$ Metal-Organic Framework. *Phys. Chem. Chem. Phys.* **2012,** *14*, 11327-11332.

(35) Getman, R. B.; Bae, Y.-S.; Wilmer, C. E.; Snurr, R. Q. Review and Analysis of Molecular Simulations of Methane, Hydrogen, and Acetylene Storage in Metal–Organic Frameworks. *Chem. Rev.* **2012,** *112*, 703-723.
(36) Boyd, P. G.; Moosavi, S. M.; Witman, M.; Smit, B. Force-Field Prediction of Materials Properties in Metal-Organic Frameworks. *J. Phys. Chem. Lett.* **2017,** *8*, 357-363.
(37) Jawahery, S.; Simon, C. M.; Braun, E.; Witman, M.; Tiana, D.; Vlaisavljevich, B.; Smit, B. Adsorbate-Induced Lattice Deformation in IRMOF-74 Series. *Nat. Commun.* **2017,** *8*, 13945.
(38) van Duin, A. C. T.; Dasgupta, S.; Lorant, F.; Goddard, W. A. ReaxFF: A Reactive Force Field for Hydrocarbons. *J. Phys. Chem. A* **2001,** *105*, 9396-9409.